

HUMAN MOTOR THALAMUS RECONSTRUCTED IN 3D FROM CONTINUOUS
SAGITTAL SECTIONS WITH IDENTIFIED SUBCORTICAL AFFERENT TERRITORIES

Igor Ilinsky^{1,3}, Perrine Paul-Gilloteaux², Pierre Gressens¹, Catherine Verney¹, Kristy Kultas-Ilinsky^{1,3}.

¹U1141 Inserm, Université Paris Diderot, Sorbonne Paris cité, UMRS 1141, Paris, France.

²UMR144, PICT IBISA Institute Curie, CNRS, Paris 75005, France; ³The University of Iowa, Iowa City, IA, 52242 USA

Acknowledgements

Authors express their gratitude to Dr. Marina Bentivoglio, Università di Verona, Verona, Italy and Dr. Alim Louis Benabid, Université de Grenoble, Grenoble, France who made their research facilities available at the initial stages of the project. The research was supported by INSERM, Université Paris Diderot, Fondation Thérèse et René Planol, and PremUp Fondation.

ABSTRACT

Classification and delineation of the motor-related nuclei in the human thalamus have been the focus of numerous discussions for a long time. Difficulties in finding consensus have for the most part been caused by paucity of direct experimental data on connections of individual nuclear entities. Recently it was found that distribution of the isoform 65 of glutamic acid decarboxylase (GAD65), the enzyme that synthesizes inhibitory neurotransmitter gamma-aminobutyric acid (GABA), is a reliable marker that allows to outline connectionally distinct nuclei in the human motor thalamus, namely the territories innervated by nigral, pallidal and cerebellar afferents. We compared these immunocytochemical staining patterns described earlier (Kultas-Ilinsky et al., 2011, J Comp Neurol, 519:2811-2837) with underlying cytoarchitectonic patterns and used the latter to outline the three afferent territories in a continuous series of sagittal Nissl-stained sections of the human thalamus. The 3D volume reconstructed from the outlines, was placed in the intercommissural line based stereotactic coordinate system and sectioned in three stereotactic planes to produce color-coded nuclear maps. This report proposes a simplified nomenclature of motor related regions and presents images of selected histological sections and stereotactic maps illustrating their topographic relationships as well as those with adjacent somatosensory afferent region. The data may become useful in different applications especially in stereotactic neurosurgery applying various imaging approaches for thalamic target identifications including diffusion tractography imaging (DTI).

SIGNIFICANCE STATEMENT

To our knowledge this report is the first demonstration of revised maps and nomenclature of human motor thalamic nuclei in three compatible stereotactic planes derived from a single brain.

The maps presented here along with histological images of sagittal sections facilitate understanding of topographical relationships of motor thalamic nuclei and adjacent structures and illustrate the magnitude of expanse of the movement-related territory in the human thalamus. The maps provide a unique tool for researchers studying human thalamus with experimental and imaging techniques as well as clinicians employing stereotactic methods for treatment and study of movement disorders.

INTRODUCTION

Longstanding controversy regarding nomenclature and delineations of so-called motor thalamic nuclei, i.e., the regions that receive basal ganglia and cerebellar input, in the human brain remains unresolved despite numerous attempts undertaken during the last decades and substantial progress achieved towards it recently (see Kultas-Ilinsky et al., 2011 and review by Mai and Forutan, 2012).

Notwithstanding its conjectural importance the issue became a focus of attention of stereotactic neurosurgeons in the middle of the last century when certain regions of the human motor thalamus became targets of neurosurgical interventions in treatment of movement disorders. Traditionally clinical neurologists utilize nomenclature by Hassler (Schaltenbrandt and Bailey, 1959; Schaltenbrandt and Wahren, 1977) where human motor thalamus consists of a great number of small cytoarchitectonic entities with unidentified functional significance and connectional specificity, which, at that time, were not as well understood as at present. At the same time clinical observations demonstrated that lesions in two Hassler's subdivisions, Vim and Vop, eliminated or significantly reduced parkinsonian tremor. It was suggested that cerebellothalamic fibers pass through and/or terminate in these regions but involvement of pallidothalamic territory was also suspected (Hassler et al., 1979).

In contrast, experimental neuroscientists working with nonhuman primates preferred to use thalamic nomenclature by Walker (1938) that was adopted in stereotactic atlas of *Macaca mulatta* by Olszewski (1952) where motor thalamus also consisted of several, but substantially fewer than Hassler's, subdivisions of three nuclei, ventral anterior (VA), ventral lateral (VL), and a part of ventral posterior (VP) connected with premotor and primary motor cortices.

Since then a large body of data has been accumulated on cortical and subcortical connections of the thalamus in pathway tracing studies in nonhuman primates and other species. These data as well as studies of immunohistochemical staining patterns led to numerous revisions of human and nonhuman thalamic nomenclatures and parcellations (Ilinsky et al., 1985; Ilinsky and Kultas-Ilinsky, 1987, 2002a,b; Hirai and Jones, 1989; Percheron et al., 1996; Macchi and Jones, 1997; Morel et al., 1997; Kultas-Ilinsky et al., 2003, 2011; Krack et al., 2002; Stepnievska et al., 1994; Calzavara et al., 2005; Jones, 2007). Nonetheless, an absence of a continuous series of cytoarchitectonic plates that illustrate topographic relationships of revised subdivisions (with the exception of the atlas of *Macaca mulatta* thalamus by Ilinsky and Kultas-Ilinsky, 2002b) has impeded a wide acceptance of proposed modifications. It is especially true with respect to the human thalamus where delineations of the nuclei, and particularly those of the most controversial motor-related subdivisions, have for the most part remained unchanged. Technical limitations involved in the work with human brain tissue and the absence of direct experimental data on distribution of subcortical afferents seem to be the main reasons.

Recently it was demonstrated that distribution patterns of glutamic acid decarboxylase isoform 65 (GAD65) in monkey and human thalami were remarkably similar, if not identical (Kultas-Ilinsky et al., 2011). Earlier numerous light and electron microscopic studies in nonhuman primates (see reviews by Ilinsky and Kultas-Ilinsky, 2001; Kultas-Ilinsky and Ilinsky, 2001) have demonstrated that thalamic territories of distribution of nigral, pallidal, and cerebellar afferents differ by type

and combination of GABA-ergic fiber and cellular components present, and this is reflected in GAD65 staining patterns specific for each territory. Thus the immunocytochemical staining for GAD65 in the human thalamus provided an indirect but reliable means for identification of the extent of projection zones of nigral, pallidal, and cerebellar afferents in this species.

In the present study we used the distribution patterns of GAD65 from Kultas-Ilinsky et al. (2011) with underlying cytoarchitectonic features of the areas to outline the three subcortical afferent territories of the human motor thalamus in continuous series of Nissl-stained sagittal sections. The outlines were used for 3D reconstruction of the thalamus. This report demonstrates selected images of computer processed sagittal sections containing motor thalamic nuclei and related color-coded maps in three stereotactic planes.

MATERIAL and METHODS

Four postmortem human brain specimens (two males and two females) perfused with 0.1M phosphate buffer followed by 4% paraformaldehyde in the same buffer used in this study were obtained from The University of Iowa Department of Anatomy Deeded Body Program. Treatment of the human tissue was in complete compliance with the guidelines of the Institutional Review Board and Human Subjects Office of the University of Iowa.

Histological Tissue Processing: Thalami with adjacent parts of midbrain and basal ganglia from both hemispheres were dissected out and postfixed in fresh fixative, 4% paraformaldehyde in 0.1M phosphate buffer (the same fixative that was used for perfusion), for a period from one to two years in a cold room. Prior to sectioning thalamic blocks were placed on a leveled horizontal surface. A hypodermic needle with a rounded sharp tip attached to a syringe, which was fixed in a stereotactic holder positioned strictly perpendicular to the horizontal surface, was driven

through the anterior (AC) and posterior (PC) commissures as they appear in the midsagittal cut to establish fiducial marks in the tissue blocks. Sagittal sections were cut on a freezing microtome MM France (Microm Microtech France, Park du Chantier, 33 Rue Bellissen 69340 Francheville, France) at 50 μ m thickness in the plane parallel to the midsagittal plane. All sections were collected and placed in individual numbered compartments to maintain the sequence. Entire section series were mounted on slides, stained with thionin and used for analysis of cytoarchitecture. Sections from the tissue block with the length of the AC-PC line, i.e., intercommissural line, of 23 mm (from one female brain) were chosen for imaging and 3D reconstruction. This length was comparable to that of the brain used for demonstration of sagittal sections in the Schaltenbrand and Bailey atlas (23.5mm) thus facilitating comparisons of coordinates of different structures in the two datasets.

The choice of the sagittal section plane was determined by the following considerations: (i) it is easier to maintain the consistency of cutting angle when sectioning in sagittal plane as compared to coronal and horizontal. This, in turn, allows more accurate comparisons of different brains; (ii) according to neuroanatomical data the projection zones of major subcortical afferent systems to the thalamus are arranged in anterior-posterior sequence, hence their topographical relationships are better appreciated in sagittal plane; (iii) landmarks of the coordinate system, i.e., positions of AC and PC in the midsagittal plane, can be easily marked and their projections easily followed in sagittal sections; (iv) total number of sagittal sections is significantly smaller than that of more frequently used coronal sections.

Image analysis and 3D reconstruction. All fifty micron thick Nissl-stained sections from the chosen tissue block were photographed with a Sony digital camera. Resulting digital images were processed in Photoshop (Adobe Systems Incorporated, 345 Park Avenue, San Jose, CA 95110) correcting the brightness and contrast and removing specks of dust and debris. Nuclear outlines

were identified in an enlarged image of one section from each group of five sections, and verified under microscope comparing with GAD65 staining pattern. Then the outlines of the sections and nuclei in them were re-traced (Figure 1A) in Adobe Illustrator (Adobe Systems Incorporated, 345 Park Avenue, San Jose, CA 95110) and aligned (Figure 1B) using fiducial marks. The set of aligned outlines was then imported as an image sequence (Rasband et al., 1997-2014) to Image J (www.imagej.nih.gov), stacked, and binarized by simple thresholding. The outlines were then closed using mathematical morphology operation called dilation to make the outlines thicker and closed, and transferred to Image J where they were filled with varying colors (Figure 2).

These color-coded images were used for 3D reconstruction. Processing was done with Amira software (FEI Software, Oregon, USA). Stacks were loaded as a 3D volume in the physical space calibrated in millimeters based on the 250 μ m section thickness and the pixel size derived from the original length of intercommissural line measured from the posterior end of AC to anterior end of PC in one of medial sections, in which the needle tracks were perfectly parallel and the outlines of the commissure markings clear. Each structure was segmented by successive 3D thresholding of each color, slightly smoothed, and converted to a 3D surface (Figure 1, C and D). The volume composed of all surfaces was rotated manually under Amira to align it within Cartesian coordinate planes in AMira physical space made visible by the creation of a reference stacks containing axes created under Matlab (the Mathworks, Massachusetts, USA). Then millimeter graduations were placed on the axes.

Volumes in cubic millimeters (Table 1) were extracted using the material measurements of Amira directly from the 3D segmented labels, and computed as the number of voxels in each volume of interest multiplied by the volume of one voxel in cubic millimeters .

To illustrate histology images of each group of five adjacent sections were merged in Adobe Photoshop resulting in 250 μm thick digital sections in which general outlines of major nuclei became more evident. The latter were further emphasized using contrast and brightness adjustments. Since the quality of the available human brain tissue was not perfect some defects during cutting were unavoidable. Merging adjacent sections helped overcome these defects and rebuild a representative image for each 250 μm (left column in Figures 3-7)

The coordinate system utilized was based on the intercommissural plane, i.e. zero horizontal plane, that passes through intercommissural line perpendicular to the midsagittal plane. A plane perpendicular to the zero horizontal plane passing through the midpoint of AC-PC line established the zero coronal plane. Distances of coronal sections posterior to the zero coronal plane and horizontal sections below the zero horizontal plane were marked with negative numbers. Mediolateral distances were measured from the midsagittal plane, i.e., midline and marked accordingly.

Nomenclature and labeling used were in principle those of Walker (1938) with some modifications concerning motor nuclei proposed by Kultas-Ilinsky et al. (2011). In this system ventral anterior nucleus (VA) defines the basal ganglia afferent territory that consists of two subdivisions – nigral afferent zone (VAn) and pallidal afferent zone (VAp). Cerebellar afferent territory is designated as ventral lateral nucleus (VL). Within it we marked its ventral region (VLv) that corresponds roughly to the part of the nucleus that was shown to display a high intensity staining for immunocytochemical marker SMI31 and is characterized by very large size neurons (Kultas-Ilinsky et al., 2011). It should be noted that individual subdivisions in some adjacent to motor thalamus nuclei labeled in the maps have not been distinguished because in many instances the exact boundaries between them were not obvious in our material like in case of subdivisions of the mediodorsal nucleus (MD). Moreover, because of profuse interdigitation

between centrolateral nucleus (CL) and the densicellular part of MD we indicated an approximate level of transition from one to another by a sharp change to a lighter density of the same color. Also due to very irregular boundary between centromedian (CM) and parafascicular nuclei (Pf) the two were assigned the same color. In the region of somatosensory afferent projections that was designated collectively as VP (ventral posterior nucleus) the two subdivisions, medial (VPM) and lateral (VPL) were also assigned the same color as the transition from one to another was not quite clear, whereas the inferior subdivision (VPI) being quite distinct, was labeled differently (see color code in Figure 2).

RESULTS

Selected digital images of Nissl-stained sagittal sections and computer generated nuclear maps at successive mediolateral levels shown in the Figure 3 illustrate the extent of the major territories of distribution of nigral, pallidal and cerebellar afferent projections in the human thalamus.

Regarding the types of nerve cells and their distribution patterns in the homologous motor thalamic nuclei there is no difference between human and rhesus monkey (Kultas-Ilinsky et al., 2011). In VL large to medium size neurons are sparsely distributed and there are numerous groups of very small cells between them. The latter are GABAergic local circuit neurons described in earlier studies. In contrast, in VAP varying size neurons, but none of them as large as in VL, are found in groups separated with passing through fiber bundles. Very small cells like the ones in VL are few. Thus cytoarchitecturally, VL and the pallidal part of VA that runs along VL for a considerable distance are distinct. This can be seen in histology images in the left column of Figure 3. The same is true for the boundary between the two VA subdivisions although in the low magnification histological images demonstrated here this may not be very obvious. Unlike VAP cells, the neurons in VAN are large and darkly stained but in contrast to VL neurons, they are

found in groups. The common feature of VAp and VAn is the rarity of very small cells. In the dorsolateral part of VAn the large neurons are smaller than in its ventromedial part but all other features are similar. Likewise large neurons of the dorsal VL are smaller than those in its ventral part.

The common VAp/VAn, and VAp /VL boundaries are very uneven with deep protrusions of cell groups of one nucleus into another. The type of material used and restrictions of image processing techniques did not allow us to demonstrate all these details in the maps. Therefore only some of this unevenness is obvious in the images of the right column of Figures 3 – 7 as well as in coronal maps in Figure 8.

The volumes of the three nuclei are shown in Table 1. The largest territory in the motor thalamus is occupied by cerebellar fiber terminals, the nigral afferent territory is the smallest. The volumes of the three motor nuclei seem to be proportional to the sizes of their afferent sources. The volumes of substantia nigra and medial globus pallidus are shown for comparison in Table 1. It should be noted that nigral afferents to the thalamus originate only from pars reticularis of substantia nigra, thus the total volume from which the nigrothalamic fibers originate is roughly two thirds of that shown in the Table 1. We do not have an appropriate figure for the volume of the deep cerebellar nuclei that are the source of cerebellar input to VL, but the massive size of the brachium conjunctivum compared to the size of ansa lenticularis and lenticular fasciculus, also seen in several images of Figures 3 – 5, leaves no doubt about the larger mass of cerebellothalamic fibers compared to pallidothalamic.

Consistent with the volume size VL has the longest medio-lateral extent of 13.5mm. Its most medial part is identifiable at 4.75 mm from the midline (Figure 3) and it ends at about 18.25 mm (Figure 7). VAp is first present at 3.75 mm but it extends only up to 16 mm from the midline. It

should be noted that at the most lateral levels it is no longer in the form of a compact entity but as scattered cell groups embedded in the VL. Only the largest of those is visible at 15.5 mm map in Figure 6. Groups of VAn neurons are identifiable slightly before 3 mm from the midline and no longer seen at 6.75 mm. The bulk of the nucleus is situated between 3.5 and 6.25 mm (Figure 3).

The ventral region of VL (VLv) separated from the rest of the nucleus by a dashed line in the maps of Figures 4 – 6 was delineated based on high intensity of staining for cytoskeletal marker SMI31 in very large neurons (Kultas-Ilinsky et al., 2011). This region takes up approximately ventral one third of VL territory and extends roughly from 7 mm to 16.25 mm from the midline. Interestingly, the very large neurons of the ventral VL extend further to its medialmost levels but these do not display the very high intensity of SMI31.

The entire motor thalamic region is situated above the zero horizontal plane as seen in the right column of Figures 3-7 and 8. Antero-posterior extent of the three nuclei varies. VAn is the shortest in anteroposterior and mediolateral dimensions and is entirely situated anterior to the zero coronal plane (Figure 8). In contrast, the bulk of VL is situated posterior to the zero coronal plane. Its anterior-posterior dimensions vary depending on the dorso-ventral coordinate. At medial levels VL is narrow ventrally, about 1mm in width, whereas dorsally in the same sections it's up to 4.0mm in width (see for example, Figure 3 bottom row). Laterally, the longest antero-posterior extent of the dorsal VL can be up to 13 mm (see for example 15 mm horizontal cut in Figure 9). The longest anteroposterior extent of VLv is 4 mm at the lateral levels starting at about 12.5 mm from the midline. VAp is situated both anteriorly and posteriorly to the zero coronal plane. At medial levels dorsal part of VAp extends up to 7 mm anterior while its ventral part extends up to 3.5 mm posterior to the zero coronal plane at some lateral levels.

The topographic relationships of the VAp and VL as well as their relationship to somatosensory complex is strikingly embodied in the horizontal plane. One can see in Figure 9 that pallidal and cerebellar territories, as well as adjacent somatosensory afferent area (shown in green) appear as consecutive bands offset relative to one another mediolaterally and at about 45 degree angle to coronal plane. In contrast, the major axis of the nigrothalamic territory is vertical as for the most part it is aligned along the mammillothalamic tract (Figures 3 and 8).

DISCUSSION

The main accomplishment of this study is a demonstration of the full extent of reliably identified human motor-related thalamic nuclei in three stereotactic planes derived from one brain. To our knowledge this is the first demonstration of this kind. Although this report shows only selected images, the entire section series through the thalamus at 250 μ m intervals with all nuclei present as well as supporting materials will be available at a later date on a dedicated internet site linked to the Society for Neuroscience database (NIF, neuinfo.org). In the present publication we discuss only major subcortical afferent zones of the motor thalamus, namely nigral, pallidal and cerebellar in the light of existing controversies and discrepancies as evidenced by publications in the fields of functional neurosurgery and brain imaging studies.

It is known from experimental studies in animals that fibers from medial globus pallidus, substantia nigra pars reticularis, and deep cerebellar nuclei reach also some other thalamic nuclei besides VAp, VAn and VL. For example, there is some nigral and cerebellar input to MD (Ilinsky et al., 1995, Mason et al., 2000) but these projections are patchy and scanty, hence not easily identifiable in the human thalamus. Cerebellar input also reaches CL, but as pointed out above its boundaries were indistinct in our material. On the other hand, in all species studied pallidal input

to CM is substantial and distributed to the entire nucleus. There is no compelling reason to believe that the same is not true for human. Moreover, practically in all types of preparations the boundaries of CM are distinct, and at lateral levels very smooth, hence no controversies have been associated with identification of this nucleus.

The nuclear outlines illustrated here encompass only major projection zones of nigral, pallidal and cerebellar afferents to the human thalamus, as accurately as it is currently possible. However, some inaccuracies may be present at the most dorsolateral boundary of VL where it borders pulvinar because the transition from one nucleus to another was not very obvious in some sections due to compromised tissue quality.

Parcellation of primate thalamus based on a large variety of immunocytochemical staining patterns has been attempted in numerous studies. In our opinion, this has worked more or less successfully only for somatosensory afferent regions. Although the functional significance of predominance of one or another antigen in a specific region remained obscure the staining patterns could be reliably correlated with modalities of peripheral somatosensory inputs (Raussel and Jones, 1991a,b; Raussel et al., 1992; Blomqwist et al., 2000). With respect to motor thalamus up until now the correlations of distribution patterns of varying immunomarkers with subcortical afferent zones have not been conclusive and have even contributed their share to existing confusion in terminology and demarcations especially in human (Jones 2007; Morel et al.1997). GAD65 staining patterns in the human motor thalamus described in detail by Kultas-Ilinsky et al. (2011) represents a step forward since they reflect directly the specifics of GABAergic circuits in the three subcortical afferent zones. Therefore GAD65 staining can be considered the most reliable marker for demarcation of three functionally different areas of the motor thalamus in human at this point of time. The nuclear maps presented here are derived from these specific staining patterns and together with proposed simplified function-related nomenclature should

provide a foundation for future parcellations within individual human motor nuclei using additional criteria when such become available.

We consider the nomenclature proposed here logical and straightforward hence easier applicable as compared to frequently referenced terminology proposed by Hirai and Jones (1989) and utilized in the atlas by Morel et al. (1997). In those the pallidal afferent territory ended up being divided between two entities, VAp and VL_a, despite that there is no substantial difference between the two either in cytoarchitecture or in various immunocytochemical staining patterns displayed. Hence their outlines vary significantly in anatomical publications while distinction between the two subdivisions in imaging studies has become even more ambiguous. Moreover, in the above two publications the dorsolateral part of the nigral afferent territory has completely vanished from the thalamus being apparently lost in one or both pallidal subdivisions. These deficiencies have recently been overcome by Mai and Forutan (2012) who based on the results of their thorough immunocytochemical analysis of human thalamus divided the anteromedial part of the motor thalamus in two subdivisions, VAl and VAm, which roughly correspond to our VAP and VAn, i.e. to pallidal and nigral territories respectively, whereas the territory they designated as VL in general coincides with the VL as defined in this study, that is cerebellar afferent territory.

One can see in Table 2 that each of the major motor nuclei outlined here encompass several Hassler's nuclear entities (see also Table 3 in Kultas-Ilinsky et al., 2011). The latter study confirmed that the human motor-related nuclei just as it has been shown in monkeys extend all the way to the dorsal boundary of the thalamus and are not confined only to its ventral part as it has been thought for some time. This removes the enigma of unknown functional role from the dorsal thalamic subdivisions in Hassler's maps (Doi, Zo, Doe, Dim, Zim, Zc). One can assert now that the dorsalmost regions of the three motor nuclei as outlined here are involved in

processing of the motor-related information derived from the basal ganglia and cerebellum just as the subdivisions ventral to them. This, of course, does not exclude the possibility of fine functional differences between dorsal and ventral parts in some or in all three nuclei, which may be due to differences in some of their cortical connections or nuances in modalities processed.

Extensive discussion in earlier neurosurgical literature concerned identification of the most effective thalamic target of stereotactic interventions for elimination of tremor (Ohye and Narabayashi, 1979; Laitinen 1985; Hirai et al., 1989; Lenz et al. 1990). The debate focused on whether the effective locus was in Hassler's Vim or Vop, at that time presumed to be cerebellar and pallidal projection zones, respectively, or in both (see review by Hamani et al., 2006). On the other hand, we found that GAD65 staining pattern in the area outlined as Vop in Hassler's maps is identical to that in the area outlined as Vim, indicating that both are part of the cerebellar afferent territory except for a narrow strip at the anterior end of Vop, which together with Voa displays staining pattern characteristic for pallidal afferent territory (Kultas-Ilinsky et al, 2011). Therefore both Vim and the bulk of Vop of Hassler are a part of VL under nomenclature applied here (Table 2), thus confirming earlier suggestions that both subdivisions represent cerebellar afferent zone (Ilinsky and Kultas-Ilinsky 2002a; Krack et al. 2002). Moreover, Vim and Vop, both form the ventral VL as marked in the maps illustrated here. According to Lenz et al. (1995) the most effective target for eliminating tremor is located in the area between 14-15 mm laterally, 2 mm anterior to the ventral posterior nucleus (VP) and 3mm above AC-PC line. As seen in the sagittal maps of Figure 3 this location is well in VLv and does not impinge on VAp. Coordinates of Vim listed in the probabilistic functional atlas by Nowinski et al. (2005) measured from the anterior end of posterior commissure also fit nicely in our VLv, although they differ from those of Lenz in dorsoventral coordinate. Likewise, the positions of tremor cells illustrated in the diagrams of Brodkey et al. (2004) fall well within VLv as outlined here. Moreover, in view of

very uneven boundary between the VL and VAp some of the points in the diagrams that scatter anterior to Vim may not be necessarily in the pallidal territory. Thus, it seems to us that finally Vim vs. Vop issue can now be considered solved.

As described in Results the topographic relationships of pallidal, cerebellar and adjacent somatosensory territories in the thalamus when viewed in horizontal cuts represent three consecutive anteroposterior bands, with their width depending on the dorso-ventral coordinate, and tilted at about 45 degrees relative to coronal and midsagittal planes. Comparing this topography with some published probabilistic maps of the thalamus constructed with DTI techniques based on cortical connectivity (see for examples Johansen-Berg et al, 2005; Mang et al., 2012; Klein et al., 2010; Kincses et al., 2012;) one can see that while the anteroposterior sequence of the zones is similar their neuroanatomical orientation, shapes, and relative sizes differ in the two datasets. The most striking and substantial difference is that the zones in those probabilistic maps are oriented mediolaterally at almost 90 degree angle to the midsagittal plane implying that they only partially overlap with subcortical afferent territories and do not accurately follow the distribution of terminals of corticothalamic fibers as known from experimental studies in nonhuman primates. The simplest explanation is the difference in the spatial resolution of the neuroanatomical and diffusion tensor imaging techniques. DTI reveals mainly the fiber bundles whereas anatomical pathway tracing and specific immunostaining patterns expose the terminal zones. Besides, both cortical and subcortical fiber bundles upon entering thalamus break up to individual fibers that take sometimes very tortuous course before reaching their final destinations (see for example individual cerebellothalamic fibers in Mason et al., 2000; and corticothalamic fibers in Kultas-Ilinsky et al., 2003). The exception are the prefrontal cortex fibers running in the anterior limb of internal capsule that stay within the bundles for some distance in the thalamus specifically when passing through VA, i.e., the basal ganglia afferent zone, *en route* to MD.

These fibers appear to be responsible for the large size of prefrontal cortex territory in the thalamus as demonstrated in most of published DT images that show it occupying the frontal one third of the thalamus throughout its entire mediolateral extent but not extending to its posterior aspect i.e. to MD nucleus.

In summary, we believe that the maps of the thalamic nuclei in three stereotactic planes demonstrated here as well as the full sets of atlas plates to be available soon will provide the common ground on which the correlation between the results of probabilistic and deterministic DT imaging studies on one hand and neuroanatomical experimental data on another can be built.

LIST OF REFERENCES

- Blomqwist A, Zhang ET, Craig AD (2000) Cytoarchitectonic and immunohistochemical characterization of a specific pain and temperature relay, the posterior portion of the ventral medial nucleus, in the human thalamus. *Brain* 123:601–619.
- Brodkey JA, Tasker RR, Hamani C, McAndrews, Dostrovsky JO, Lozano AM (2004) Tremor cells in the human thalamus: Differences among neurologic disorders. *J Neurosurg* 101:43-47.
- Calzavara R, Zappala A, Rozzi S, Matelli M, Luppino G (2005) Neurochemical characterization of the cerebellar-recipient motor thalamic territory in the macaque monkey. *Eur J Neurosci* 21:1869–1894.
- Hamani C, Dostrovsky JO, Lozano AM (2006) The motor thalamus in neurosurgery. *Neurosurgery* 58:146-158.
- Hassler R, Mundinger F, Riechert T (1979) *Stereotaxis in Parkinson Syndrome*. Heidelberg: Springer Verlag.
- Hirai T, Jones EG (1989) A new parcellation of the human thalamus on the basis of histochemical staining. *Brain Res Rev* 14:1–34.
- Hirai T, Ohye C, Nagaseki Y, Matsumura M (1989) Cytometric analysis of the thalamic ventralis intermedialis nucleus in humans. *J Neurophysiol* 61:478-487.
- Ilinsky IA, Jouandet ML, Goldman-Rakic PS (1985) Organization of the nigrothalamocortical system in the rhesus monkey. *J Comp Neurol* 236:315–330.

Ilinsky IA, Kultas-Ilinsky K (1987) Sagittal cytoarchitectonic maps of the *Macaca mulatta* thalamus with a revised nomenclature of the motor-related nuclei validated by observation of their connectivity. *J Comp Neurol* 262:331–364.

Ilinsky IA, Kultas-Ilinsky K (2001) Neuroanatomical organization and connections of the motor thalamus in primates. In: *Basal Ganglia and Thalamus in Health and Movement Disorders*. (Kultas-Ilinsky K, Ilinsky IA eds), pp.77-91. New York, Boston, Dordrecht: Kluwer/Academic/Plenum Publishers

Ilinsky I, Kultas-Ilinsky K (2002a) Motor thalamic circuits in primates with emphasis on the area targeted in treatment of movement disorders. *Mov Disord* 17 (Suppl 3): S9–S14.

Ilinsky IA, Kultas-Ilinsky K (2002b) Stereotactic atlas of *Macaca mulatta* thalamus and adjacent basal ganglia nuclei. New York: Kluwer/Academic/Plenum Publishers.

Johansen-Berg H, Behrens TEJ, Sillery E, Ciccarelli O, Thompson AJ, Smith SM, Matthews PM (2005) Functional-anatomical validation and individual variation of diffusion tractography-based segmentation of the human thalamus cerebral cortex 15:31– 39.

Jones EG (2007) *The Thalamus*, 2nd ed. pp.1396–1451. New York: Cambridge University Press.

Kincses ZT, Szabó N, Valálik I, Kopniczky Z, Dézsi L, Klivényi P, Jenkinson M, Király A, Babos M, Vörös E, Barzo P, Vécsei L (2012) Target Identification for Stereotactic Thalamotomy Using Diffusion Tractography. *PLoS ONE* 7(1): e29969. doi:10.1371/journal.pone.0029969.

Klein JC, Rushworth MFS, Behrens TEJ, Mackay CE, de Crespigny AJ, D'Arceuil H, Johansen-Berg H (2010) Topography of connections between human prefrontal cortex and mediodorsal thalamus studied with diffusion tractography. *NeuroImage* 51:555–564.

Krack P, Dostrovsky J, Ilinsky I, Kultas-Ilinsky K, Lenz F, Lozano A, Vitek J (2002) Surgery of the motor thalamus: problems with the present nomenclatures. *Mov Disord* 17 (Suppl 3):S2–S8.

Kultas-Ilinsky K, Ilinsky IA (2001) Neurotransmitters and receptors in the primate motor thalamus and potential for plasticity. In: *Basal Ganglia and Thalamus in Health and Movement Disorders*. (Kultas-Ilinsky K, Ilinsky IA eds), pp.215-224. New York, Boston, Dordrecht: Kluwer/Academic/Plenum Publishers.

Kultas-Ilinsky K, Sivan-Loukianova E, Ilinsky IA (2003) Re-evaluation of the primary motor cortex connections with the thalamus in primates. *J Comp Neurol* 457:133-158.

Kultas-Ilinsky K, Ilinsky IA, Verney C. (2011) Glutamic acid decarboxylase isoform 65 immunoreactivity in the motor thalamus of humans and monkeys: γ -aminobutyric acidergic connections and nuclear delineations. *J Comp Neurol* 519:2811–2837.

Laitinen LV (1985) Brain targets for Parkinson's disease: results of a survey of neurosurgeons. *J Neurosurg* 62:340-351.

Lenz FA, Kwan HC, Dostrovsky JO, Tasker RR, Murphy JT, Lenz YE (1990) Single unit analysis of the human ventral thalamic nuclear group. Activity correlated with movement. *Brain* 113:1795-1821.

Lenz FA, Normand SL, Kwan HC, Andrews D, Rowland LH, Jones MW, Seike M, Lin YC, Tasker RR, Lenz YE (1995) Statistical prediction of the optimal site for thalamotomy in Parkinsonian tremor. *Mov Dis* 10:318-328.

Macchi G, Jones EG (1997) Toward an agreement on terminology of nuclear and subnuclear divisions of the motor thalamus. *J Neurosurg* 86:670-685.

Mai JK, Forutan F (2012) Thalamus. In: *The Human Nervous System*, 3d edition, pp.618-676. Amsterdam: Elsevier.

Mang SC, Busza A, Reiterer S, Grodd W, Klose U (2012) Thalamus segmentation based on the local diffusion direction: A group study. *Magn Reson Med* 67:118-126.

Mason A, Ilinsky I, Maldonado S, Kultas-Ilinsky K. (2000) Thalamic terminal fields of individual axons from the ventral part of the dentate nucleus of the cerebellum in *Macaca mulatta*. *J Comp Neurol* 412:412-428.

Morel A, Magnin M, Jeanmonod D (1997) Multiarchitectonic and stereotactic atlas of the human thalamus. *J Comp Neurol* 387:588–630.

Nowinski WL, Belov D, Thiravanukarasu A, Benabid AL (2005) A probabilistic functional atlas of the VIM nucleus constructed from pre-, intra- and postoperative electrophysiological and neuroimaging data acquired during the surgical treatment of Parkinson's disease patients. *Stereotact Funct Neurosurg* 83: 190-196.

Ohye C, Narabayashi H (1979) Physiological study of presumed ventralis intermedius neurons in the human thalamus. *J Neurosurg* 50:290-297.

Olszewski J (1952) *The thalamus of Macaca mulatta*. An atlas for use with the stereotaxic instrument. New York: Karger.

Percheron G, Francois C, Talbi B, Yelnik J, Fenelon G (1996) The primate motor thalamus. *Brain Res Rev* 22:93-181.

Rasband, WS (1997-2014) ImageJ, U. S. National Institutes of Health, Bethesda, Maryland, USA

Raussen E, Jones EG (1991a) Histochemical and immunocytochemical compartments of the thalamic VPM nucleus in monkeys and their relationship to the representation map. *J Neurosci* 11:210-225.

Raussen E, Jones EG (1991b) Chemically distinct compartments of the thalamic VPM nucleus in monkeys relay principal and spinal trigeminal pathways to different layers of the somatosensory cortex. *J Neurosci* 11:226-237.

Raussel E, Bae CS, Vinuela A, Huntley GW, Jones EG (1992) Calbindin and Parvalbumin Cells in monkey VPL thalamic nucleus: distribution, laminar cortical projections, and relations to spinothalamic terminals. *J Neurosci* 12:4088-4111.

Schaltenbrandt G, Bailey P (1959) Einführung in die stereotaktischen Operationen mit einem Atlas des menschlichen Gehirns. Stuttgart: Thieme.

Schaltenbrandt G, Wahren W (1977) Atlas for stereotaxy of the human brain. Stuttgart: Thieme.

Stepnievska I, Preuss T, Kaas J (1994) Architectonic subdivisions of the motor thalamus of owl monkeys: Nissl, acetylcholinesterase, and cytochrome oxidase patterns. *J Comp Neurol* 349:536-557.

Walker AE (1938) The Primate Thalamus. Chicago: Chicago University Press.

FIGURE LEGENDS

Figure 1. Illustration of consecutive stages of image processing. **A** – example of nuclear outlines traced from 50 μ m thick section. **B** – Example of a group of aligned outlines. **C** – A group of outlines with thickness added. **D** –medial view of 3D reconstructed volume of color-coded structures. Positions of coordinate planes are indicated with the two perpendiculars: horizontal axis indicates position of the intercommissural plane, i.e., zero horizontal plane, vertical axis shows the position of the zero frontal plane.

Figure 2. Color Code and Nuclear Abbreviations

Figure 3. Examples of sagittal histological images and color-coded maps. To illustrate the medio-lateral extent of the three motor nuclei this and the following four figures (Figures 4 –7) show selected images of the series of sagittal computer-processed Nissl-stained sections (left column) and corresponding sagittal cuts of reconstructed 3D volume with color-coded nuclei (right column) at different distances from the midline. The distances of each pair of images from the midline are indicated between them. This panel illustrates sections from 3.25 to 6mm from

the midline. VAn – dark purple, VAp – dark blue, and VL – bright yellow. For labeling of all other nuclei see color code in Figure 2.

Figure 4. Examples of sagittal histological images and color-coded maps. Continuation of the series shown in Figure 3 representing the level from 7.25 to 9 mm from the midline. The black dashed contour in VL indicates the approximate dorsal boundary of VLv. Groups of cells in adjacent motor nuclei reach significantly into each other territories making the boundary between them very uneven. Despite the low contrast this can be noticed in histological images in the left column. These zigzag are smoothed in 3D volume due to technical limitations. The rest of the labeling as in Figure 3.

Figure 5. Examples of sagittal histological images and color-coded maps. Continuation of the series shown in Figures 3 and 4 representing level from 10.75 to 13.5 mm from the midline. Labeling as in Figures 3 and 4.

Figure 6. Examples of sagittal histological images and color-coded maps. Continuation of the series shown in Figures 3, 4 and 5 representing the level from 14.5 to 16.75 mm from the midline. Labeling as in Figures 3 – 5.

Figure 7. Examples of sagittal histological images and color-coded maps. Continuation of the series shown in Figures 3 – 6 showing the most lateral extension of VL at 18.25 mm from the midline. Labeling as in Figures 3 – 6.

Figure 8. Examples of coronal maps derived from the reconstructed 3D volume. The cut at zero coronal plane (0mm) is shown in the second image from the right in the second row. Cuts posterior to the coronal plane are marked with negative (-) numbers. Vertical axis indicates the midsagittal plane, horizontal axis – the zero horizontal plane.

Figure 9. Examples of horizontal maps from the reconstructed 3D volume. All levels shown are above the zero horizontal plane as the motor nuclei do not extend below it. The cut at the zero level, i.e., at the CA-CP plane, is in the bottom of the right column (0.0mm). Horizontal axis shows the position of the midline. Vertical axis indicates position of the zero coronal plane.

Figure 1

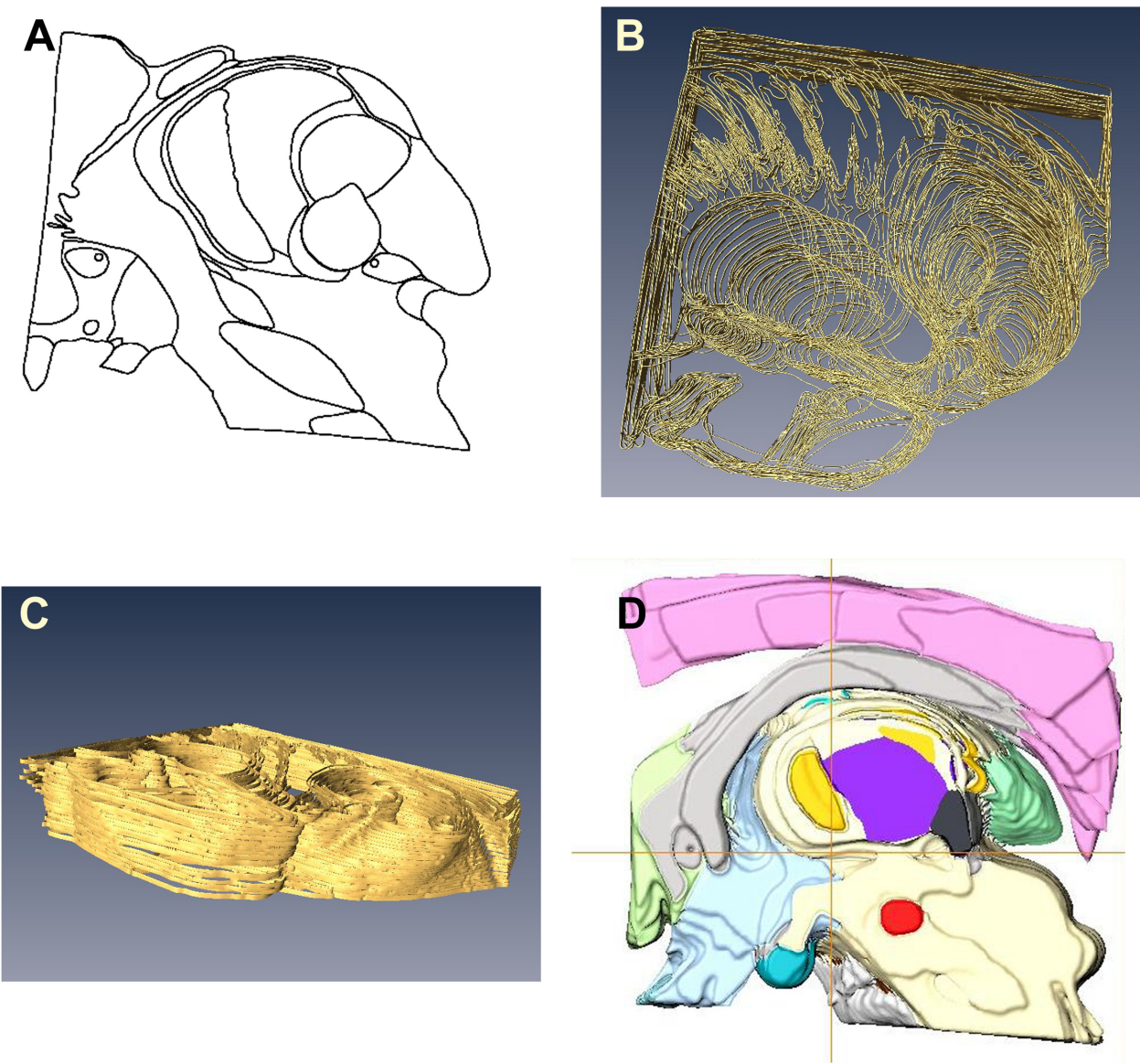


Figure2

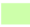





















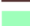

















Brain regions	
	Basal Forebrain
	Hypothalamus
	Midbrain
Nuclei	
	A - Anterior
	Cd/Put/VSt - Caudate/Putamen/ Ventral Striatum
	CM/Pf - Centromedian/Parafascicular
	GPI - Globus Pallidus lateral
	GPm - Globus Pallidus medial
	HbL - Habenula lateral
	Hbm - Habenula medial
	LD - Laterodorsal
	LG - Lateral Geniculate
	Li - Limitans
	MB - Mammillary Body
	MD- mediodorsal
	MD/CL - Mediodorsal/Centrolateral
	M - Meynert's nucleus
	MGC - MG complex
	MG - Medial geniculate
	MI - Midline
	PC -Paracentral
	PPN - Pedunculopontine
	Po - Pontine
	Pul - Pulvinar
	R - Red
	Rt - Reticular
	Sch - Suprachiasmatic
	SN - Substantia nigra
	STN - Subthalamic
	VAn - Ventral Anterior nigral
	VAp - Ventral Anterior pallidal
	VLd/VLv - Ventral Lateral dorsal/medial
	VPI - Ventral Posterior inferior
	VPI/VPm - Ventral Posterior lateral/medial
Fiber Tracts	
	al - ansa lenticularis
	fr - fasciculus retroflexus
	fx - fornix
	mt - mamillothalamic tract
	pc - posterior commissure
	ac - anterior commissure
	bc - brachium conjunctivum
	bsc - brachium of superior colliculus
	ic - internal capsule
	eml - external medullay lamina
	lf - lenticular fasciculus
	ot - optic tract

Figure 3

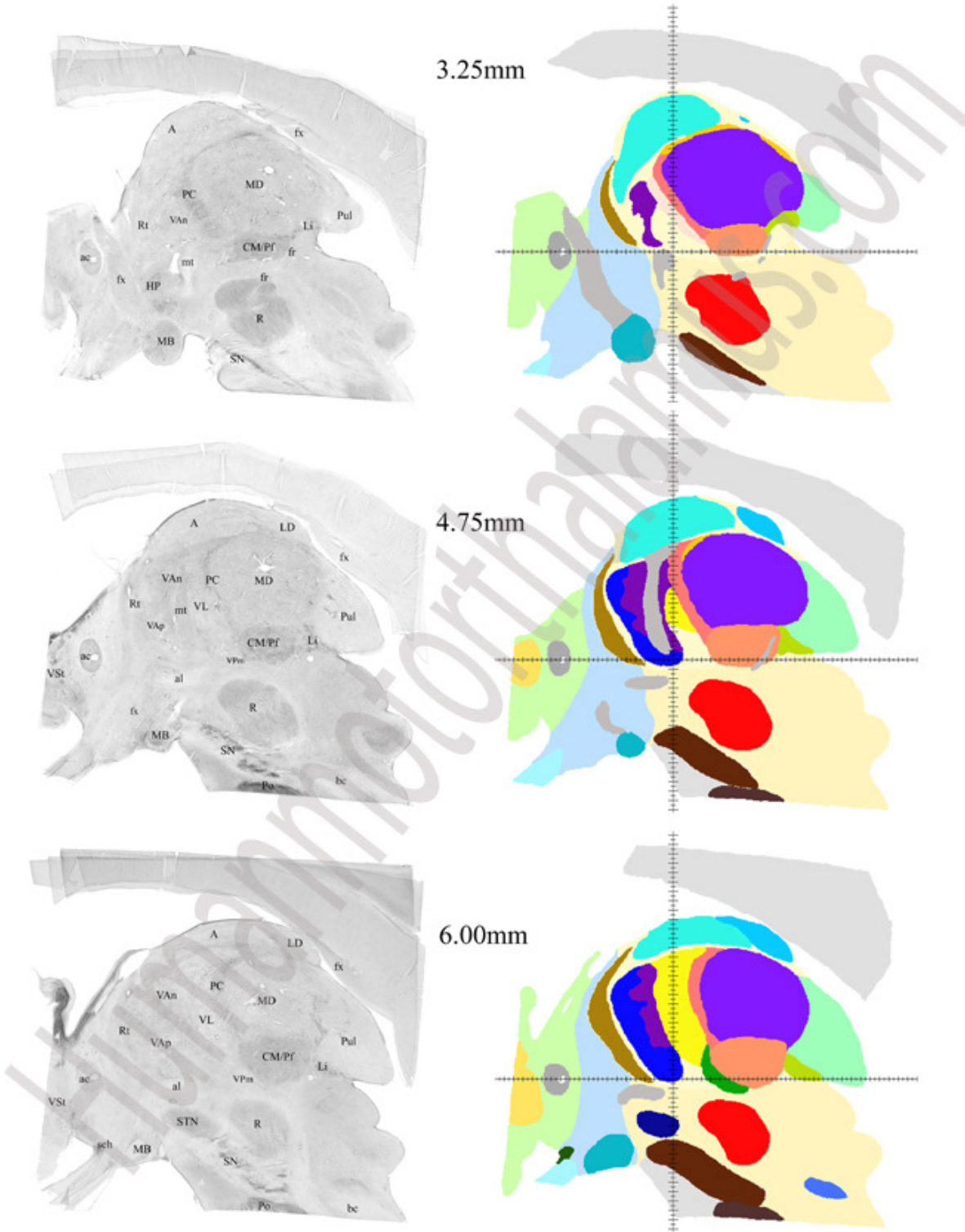


Figure 4.

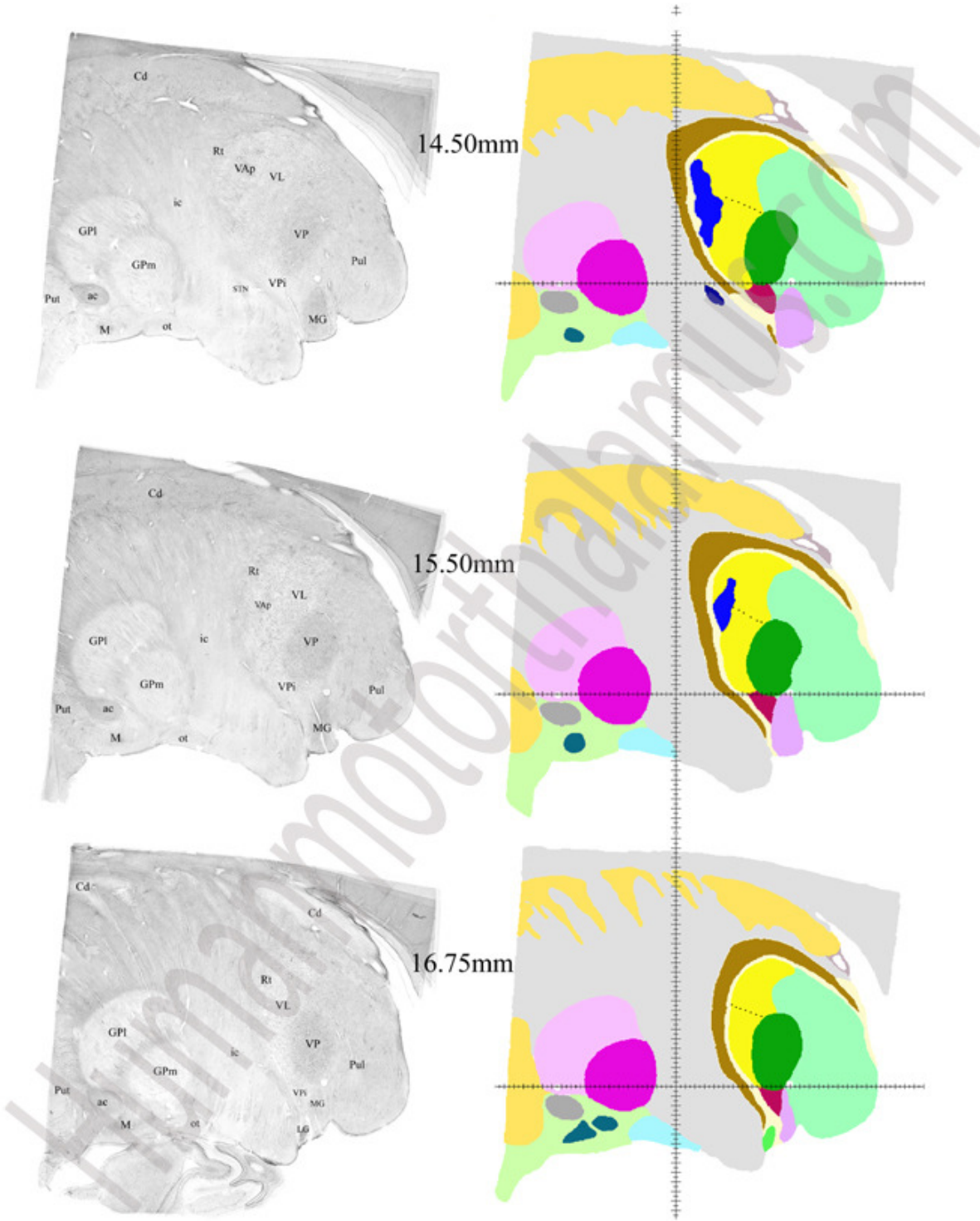


Figure 5.

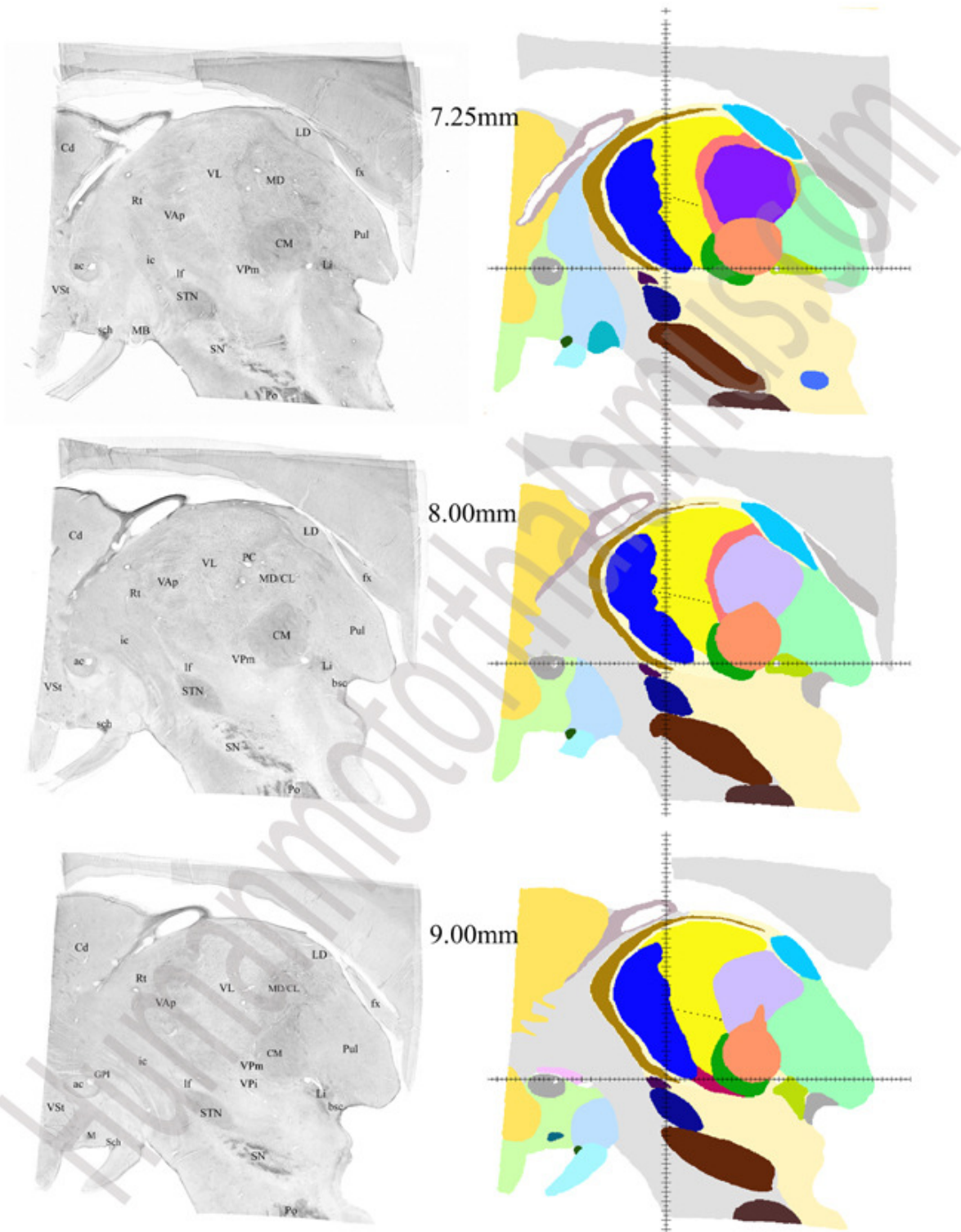


Figure 6.

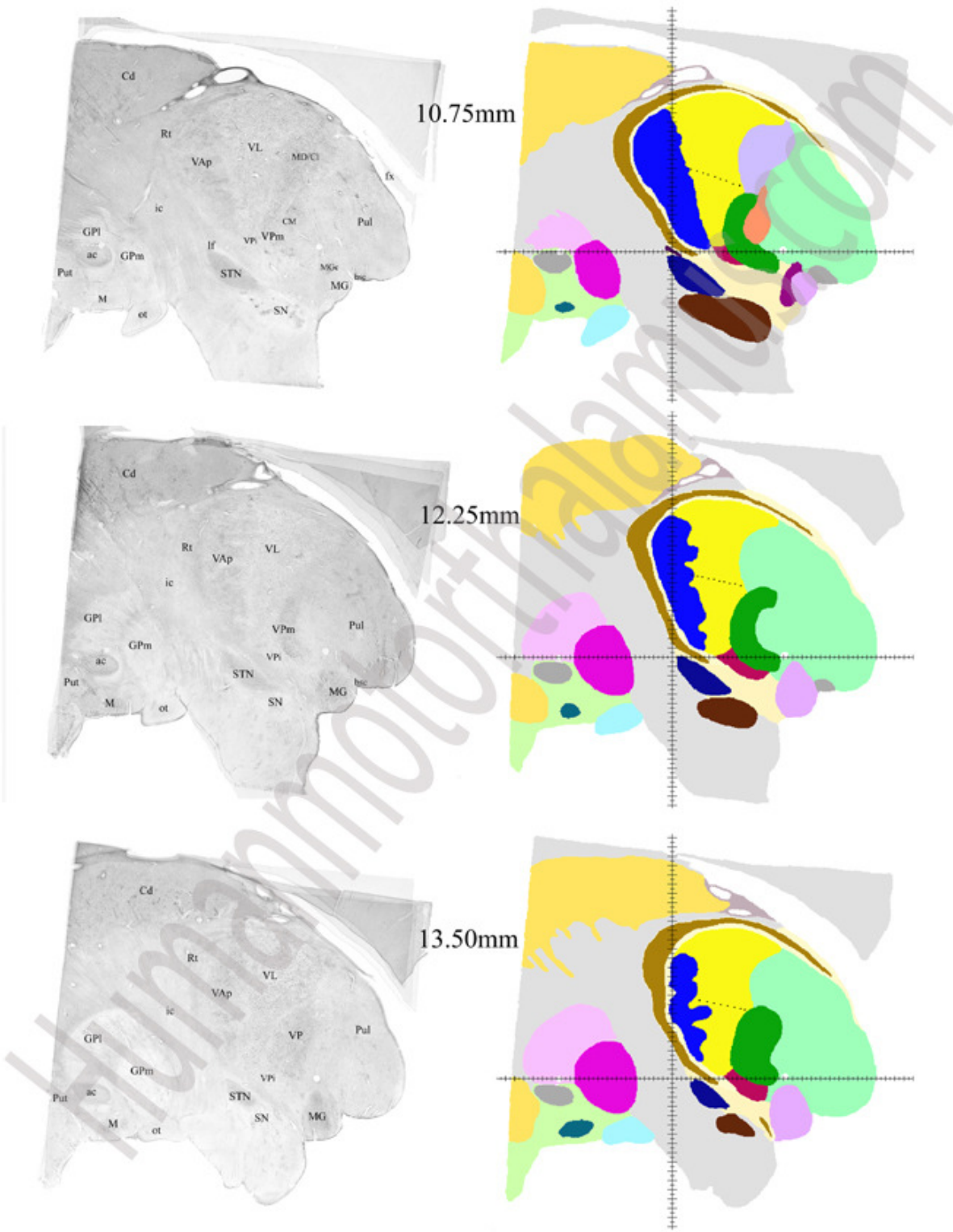


Figure 7.

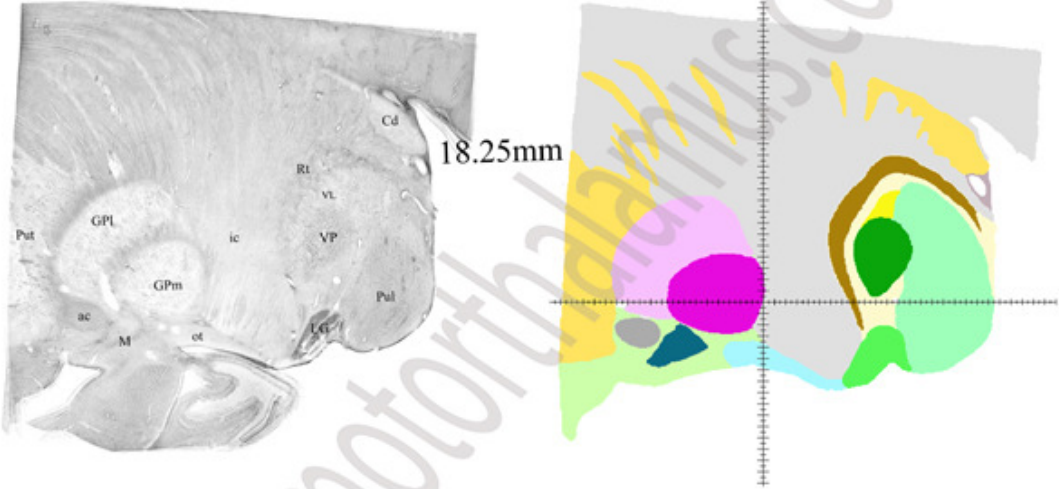


Figure 8

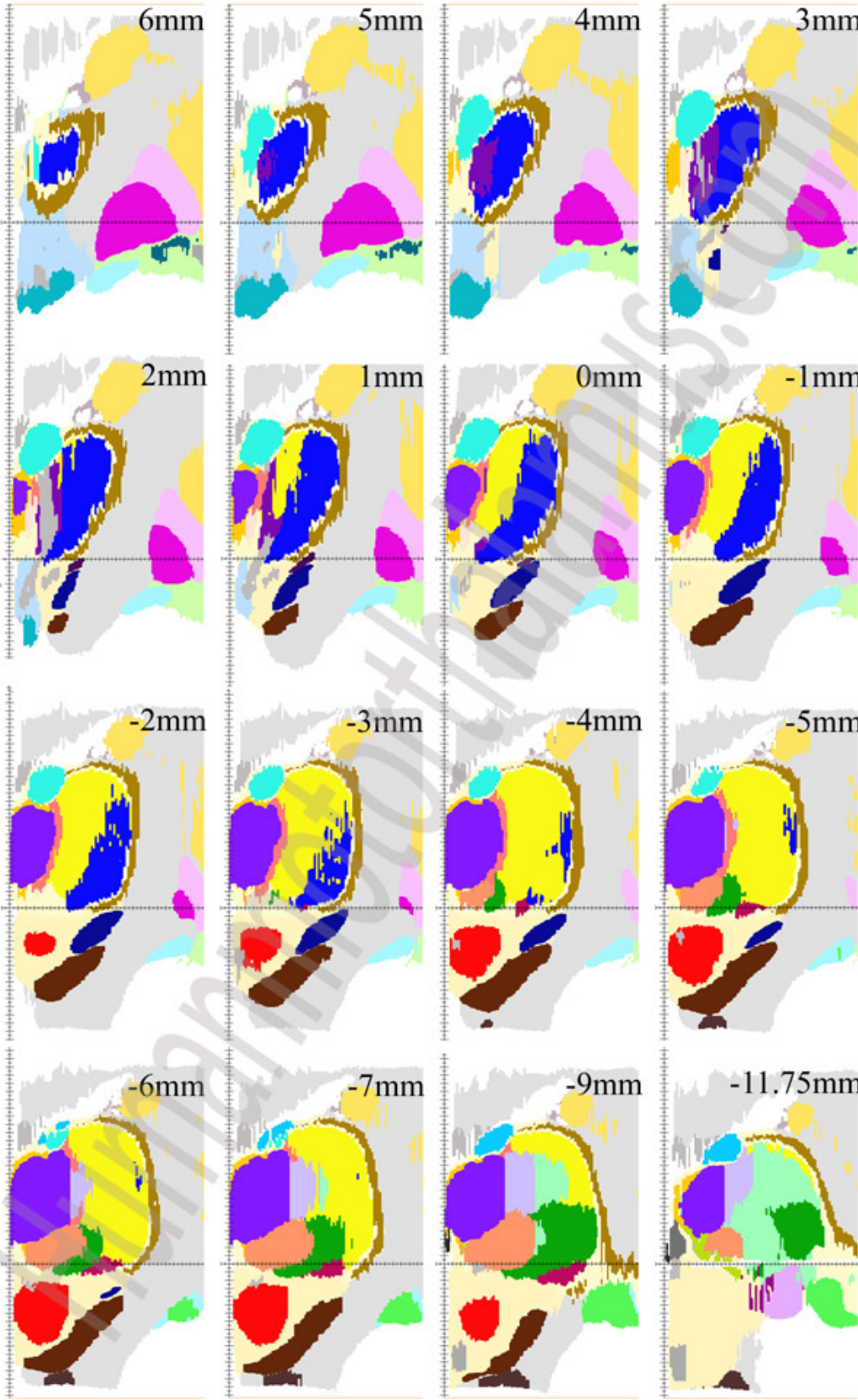


Figure 9.

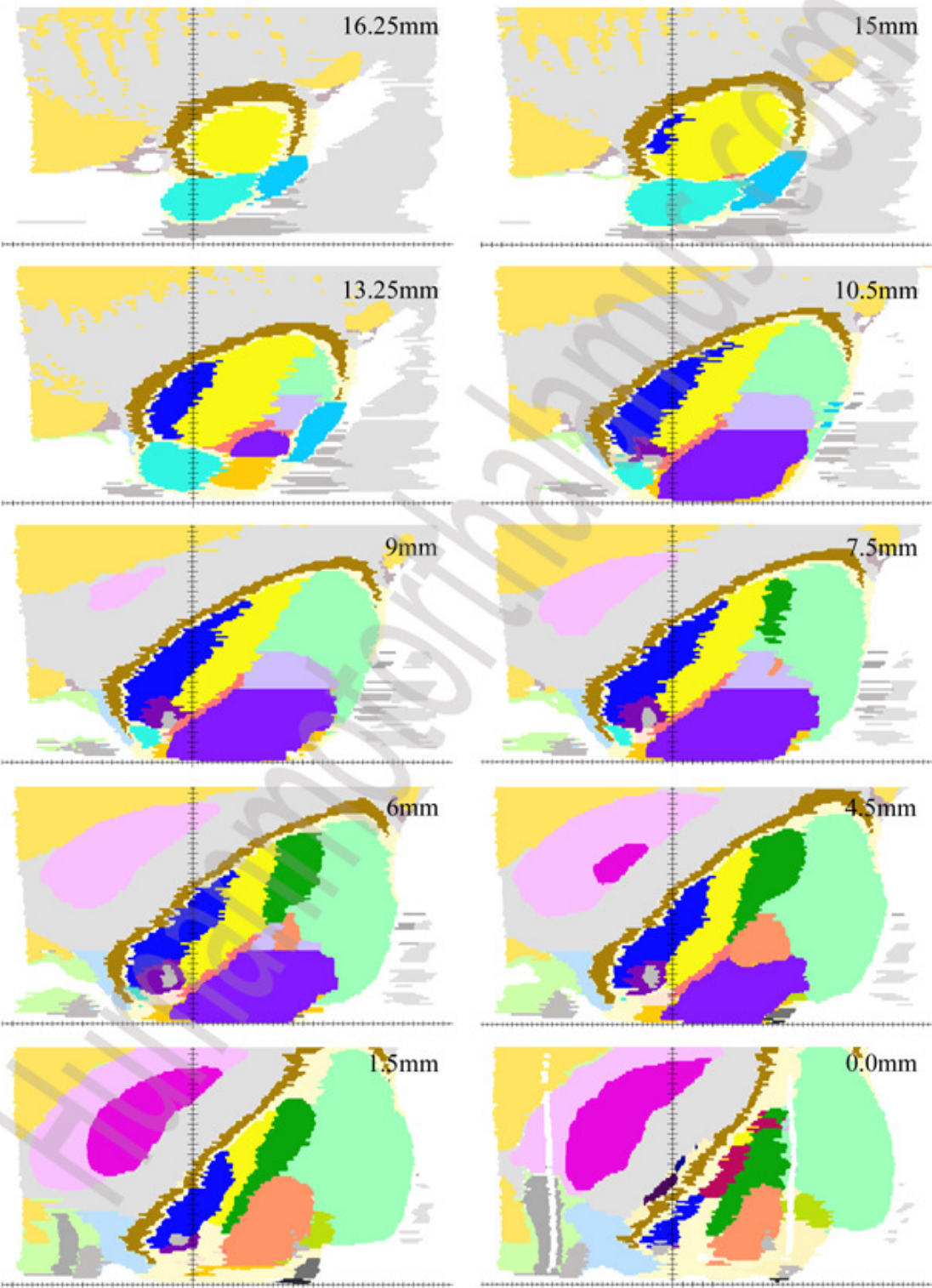


Table 1. Volumes of Human Motor- Related Thalamic Nuclei and Sources of their afferent inputs.

Nuclei	Volume in mm³
VAn	68.38
VAp	457.15
VL (VLd andVLv)	843.59
Substantia Nigra	344.65
Medial Globus Pallidus	495. 81
Deep Cerebellar Nuclei	Not available

Table 2. Comparison of classifications of human motor-related thalamic nuclei of this study and that of Hassler (1959).

Subcortical afferent sources	Nuclear subdivisions of this study	Corresponding nuclear subdivisions of Hassler
Substantia nigra pars reticularis	VAn	Lpo.mc, and parts of Lpo and Doi,
Medial globus pallidus	VAp	Voa, marginally Vop, parts of Lpo, Doi, Zo, Doe, and Voi
Deep cerebellar nuclei	VL (VLd and VLv)	Vim, bulk of Vop, and parts of Voi, Vom, Dim, Doi, Zim, Zo, and Zc

Key words: stereotactic maps, motor thalamic nuclei, VIM, 3D reconstruction, human thalamic nomenclature, DT imaging.